Extended Abstracts of the 2001 International Conference on Solid State Devices and Materials, Tokyo, 2001, pp. 236–237

LB-2-2

Antimony Behavior in Laser Annealing Process for Ultra Shallow Junction Formation

K. Shibahara, Y. Ishikawa, D. Onimatu, N. Maeda, A. Mineji*, K. Kagawa**, A. Matuno**, T. Nire**

Research Center for Nanodevices and Systems, Hiroshima University,
* NEC ULSI Device Development Division, **Research Center, Research Division, Komatsu Ltd.
1-4-2 Kagamiyama, Higashi-Hiroshima, 739-8527, Japan
Phone: +81-824-24-6265, Fax: +81-824-22-7185, e-mail: shiba@sxsys.hiroshima-u.ac.jp

1. Introduction

Laser annealing (LA) is known as the effective method for shallow junction formation. It is recently attracted for B activation to improve activation rate and sheet resistance by very short time non-thermal-equilibrium annealing [1,2]. In contrast to B, LA of donor impurities has not been investigated well, in spite that both p- and n- types regions are annealed simultaneously in CMOS device fabrication. We have reported ultra shallow and low resistive junctions formation by Sb^+ implantation using furnace annealing and rapid thermal annealing (RTA) methods [3-5]. In this report, evaluation of laser annealed Sb^+ implanted layers are described.

2. Experiment

Antimony was implanted into Si (100) substrates with a 5-nm-thick screen oxide. Implantation energy and dose were 10 keV and 6×10^{14} cm^{-2}, respectively. KrF excimer laser whose wave length was 248 nm and pulse width was 38 ns was used for laser annealing. Laser energy density was changed in the range of 600 mJ/cm^2 to 800 mJ/cm^2. Laser pulse was repeatedly irradiated to some specimens to observe variations due to multi-times LA. The screen oxide used for the Sb^+ implantation was left as it was for LA. Though thicker oxides are sometimes utilized as an anti-reflective film for the laser annealing, they sometimes give rise to surface roughening as shown in Fig. 1. In the case of the 5 nm oxide, such roughening was not observed.

3. Results and Discussion

Figures 2 (a) and 2 (b) show oxygen and Sb SIMS depth profiles for single pulse LA, respectively. The junction depths except for the laser energy density of 800 mJ/cm^2 case, defined by the Sb concentration of 1×10^{18} cm^{-3}, are about 20 nm. This value is almost same as that for the as implanted case. Wide spreading of Sb for the 800 mJ/cm^2 case is considered to originate from melting of crystalline Si, since diffusion in melted Si is much faster than that in solid Si. Another noteworthy feature concerning melting is oxygen pileup peaks in Si. Oxygen tails in Si is attributed to knock-on of the screen oxide during Sb^+ implantation and no pileup peak is observed in the as implanted oxygen profile. The peaks at 9.5 nm from the screen oxide/Si interface are found for 600 and 700 mJ/cm^2. This depth is coincident with thickness of the amorphous layer formed by Sb^+ implantation. The amorphous layer thickness was estimated using our previous result [6]. In the cross-sectional transmission electron microscopy (TEM) photograph shown in Fig. 3, many stacking faults whose depths are nearly 10 nm are observed. The oxygen peak in Fig. 2 (b) moves to 22 nm depth for 800 mJ/cm^2. The phenomena described here are interpreted as follows. At lower laser density condition, only the surface amorphous layer melts because of its lower melting point than crystalline Si. Small difference in the laser density dose not affect melting depth as long as the crystalline Si temperature during LA is lower than its melting point. The oxygen existing in Si segregates at the melting interface as a silicon oxide precipitation. The oxide precipitation works as a seed of stacking faults and can be observed by SIMS analysis as a pileup. Therefore, the oxygen pileup peak can be utilized as a melting zone marker.

Antimony pileup at the screen oxide/Si interface in Fig. 2 (a) is also attributed to melting. Since Sb non-thermal-equilibrium segregation coefficient at the melt/crystal interface is lower than other dopants, Sb transport towards the surface by recrystallization is comprehensive.

Because of Sb redistribution behavior caused by the melting, high laser energy density annealing is not preferable for Sb. Therefore, effects of multi pulses LA are investigated. Figures 4 and 5 show Sb SIMS depth profiles for sub-crystal-melt condition where the amorphized layer melts and recrystallized by the first laser pulse. In the cases of 600 and 650 mJ/cm^2, amounts of retained Sb estimated from the SIMS profile increase as LA pulse number increases. That tendency is reflected to decrease in sheet resistance shown in Fig. 6. The increase in retained Sb probably results from redistribution of the pileup Sb at the screen oxide/Si interface into Si. In spite of the lowest retained Sb amount, the sheet resistance for 700 mJ/cm^2 is lowest. Improvement in dopant activation due to increase in the laser density and thermal budget is possible origin of this result. The sheet resistance for 700 mJ/cm^2 once decreases and then increases by repeating LA. As shown in Fig. 5, junction depth becomes deeper for this laser density, Sb deactivation due to precipitation is considerable origin of increase in the sheet resistance. Though the minimum sheet resistance value obtained by LA is comparable to that for RTA as shown in Fig. 6, further improvement seems to be possible by optimizing the combination of the laser energy density and the pulse number.

4. Summary

Laser annealing of Sb^+ implanted Si for shallow junction formation has been investigated. Phenomena relating to Si melting are discussed by using the oxygen pileup as a marker. Sheet resistance was conditionally improved by repeating LA on laser energy density.

References

[1] B. Yu, et al., IEDM Tech. Digest, p.509 (1999).
[2] K. Goto, et al, IEDM Tech Digest, p.931 (1999).
[3] K. Shibahara, et al, Extend. Abst. SSDM p.314 (1999).
[4] K. Shibahara, et al, Jpn. J. Appl. Phys. **39** p.2194 (2000).
[5] K. Shibahara, et al, Mat. Res. Soc. Symp. Proc **610** p.B8.5.1 (2000).
[6] K. Shibahara, et al, Mat. Res. Soc. Symp. Proc. **532** p.23 (1998).

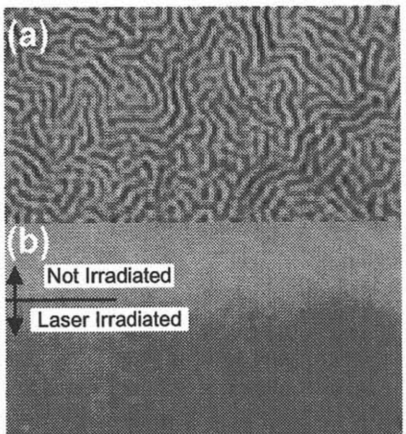

Fig. 1 Nomarski optical micrograph of specimens' surface after LA. Specimens were covered by 20 nm (a) and 5 nm (b) oxides, respectively. Surface roughening observed for thick oxide cases is not observed for the 5 nm oxide case.

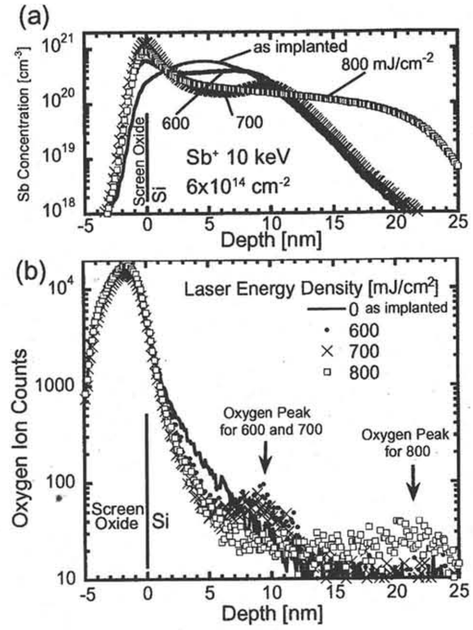

Fig. 2 SIMS depth profiles of Sb (a) and oxygen (b). After LA, oxygen shows pileup which is probably attributed to oxide precipitation at the melted and unmelted regions interface. Junction depths are about 20 nm as long as the melted region does not spread to deep inside of Si.

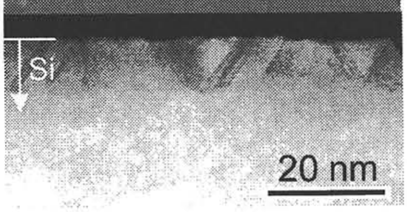

Fig. 3 Cross-sectional TEM micrograph of a laser annealed specimen. A lot of stacking faults exist in the surface-10-nm-depth layer which was an originally amorphized layer formed by Sb^+ implantation . A screen oxide was removed prior to TEM observation.

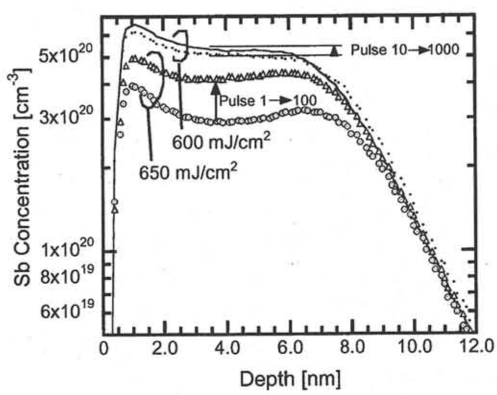

Fig. 4 Variations in Sb SIMS depth profiles due to increase in laser pulse numbers. Retained Sb in Si increases as the pulse number increases. Diffusion of Sb is negligible for 600 and 650 mJ/cm2 laser pulses. The screen oxide was removed prior to SIMS measurement.

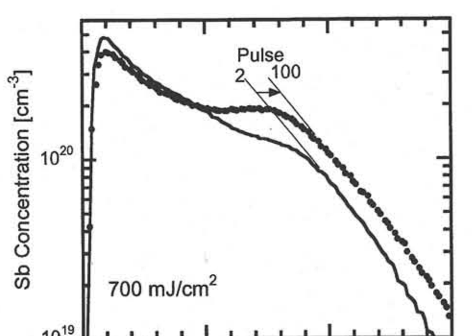

Fig. 5 Antimony SIMS depth profiles for 700 mJ/cm² laser pulses. Differently from the 600 and 650 mJ/cm² cases, Sb diffusion due to repeated laser irradiation is clearly observed. The screen oxide was removed prior to SIMS measurement.

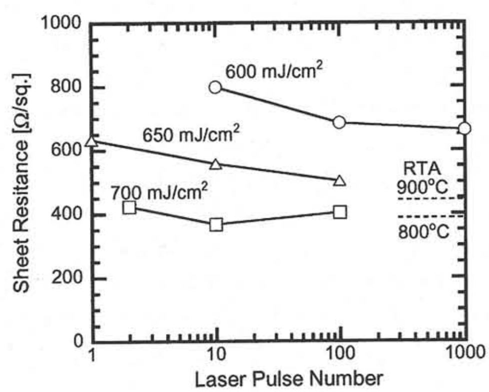

Fig. 6 Relationships between the laser pulse number and sheet resistance of the Sb^+ implanted layers. The sheet resistance was measured by two points probe method. The sheet resistances for 600 and 650 mJ/cm² shows monotonous reduction against the pulse numbers. In the case of 700 mJ/cm², the sheet resistance increases for the 100 pulses after decrease for the 10 pulses.

Table 1 Variation of retained Sb in Si by increasing a laser pulse number. Retained Sb shows increase by repeated laser irradiation for all cases.

	Retained Sb
600 mJ/cm², Pulse 10 → 1000	4.6×10^{14} cm^{-2} → 4.7×10^{14} cm^{-2}
650 mJ/cm², Pulse 1 → 100	3.0×10^{14} cm^{-2} → 3.9×10^{14} cm^{-2}
700 mJ/cm², Pulse 2 → 100	2.3×10^{14} cm^{-2} → 2.4×10^{14} cm^{-2}